Scientific Research Publishing

Materials Sciences and Applications, 2023, 14, 336-345
https://www.scirp.org/journal/msa
ISSN Online: 2153-1188
ISSN Print: 2153-117X

# Welding Effect at the Heat Affected Zone by Joining a Gray Cast Iron with Stainless Steel E308-16

**Yajaira Curiel-Razo[1], Enrique Curiel-Reyna[1], Minerva Robles-Agudo[2], Alberto Lara-Guevara[3], Ignacio Rojas-Rodríguez[2*]**

[1]Facultad de Estudios Superiores-Cuautitlán, Universidad Nacional Autónoma de México, Cuautitlán-Izcalli, México
[2]División Industrial, Universidad Tecnológica de Querétaro, Querétaro, México
[3]División de Posgrado, Facultad de Informática, Universidad Autónoma de Querétaro, Querétaro, México
Email: *irojasmx@yahoo.com.m

**How to cite this paper:** Curiel-Razo, Y., Curiel-Reyna, E., Robles-Agudo, M., Lara-Guevara, A. and Rojas-Rodríguez, I. (2023) Welding Effect at the Heat Affected Zone by Joining a Gray Cast Iron with Stainless Steel E308-16. *Materials Sciences and Applications*, **14**, 336-345.
https://doi.org/10.4236/msa.2023.146021

**Received:** May 16, 2023
**Accepted:** June 23, 2023
**Published:** June 26, 2023



## Abstract

Different investigations of the union of dissimilar materials such as stainless steel and different castings have been carried out, but rapid cooling immediately after welding has not been considered, in this work it was investigated how rapid cooling affects the metallurgical microstructure and consequently the mechanical properties. The effect of welding parameters on the microstructure and mechanical properties of the joint between dissimilar metals, an E-308-16 austenitic stainless steel and Gray Cast Iron was also analyzed. Gray cast iron samples (GCI) were fabricated, welded and cooled. The main welding parameters studied in this work are the welding technique and the type of filler electrodes. Flux-coated electrode E-308-16 was applied for this different joint. An experimental study was carried out for the analysis of welded joints of similar and dissimilar steels. The microstructure of the welded joints was analyzed using an optical microscope, in the base metals, heat affected zone (HAZ) and filler metal. The mechanical properties of the welded joints were evaluated by Vickers microhardness and tensile strength tests. The hardness profile showed differences in hardness between the base metals, the heat affected zone and the filler metal. The metallurgical microstructures observed along the welded areas corresponded to the profile. The hardness differences determined the effect on the mechanical and metallurgical characteristics of the welded samples as a result of the cooling rate differences. This research work is important because it allows us to analyze the possibility of reworking pieces of dissimilar materials by welding or, failing that, to determine if this may or may not be possible.

**Keywords**

Gray Iron, Welding, Hot Affected Zone, Filler Metal, Microstructure, Dissimilar Metals

## 1. Introduction

One of the recent challenges in modern industry is to simplify component design by welding different materials. Characteristics and properties such as strength, corrosion resistance and low maintenance cost should be considered for different cast iron to stainless steel joints in different applications, such as the welding of cast iron couplings to stainless steel pipes [1].

Some metals are easily weldable, but others are difficult to weld, requiring specific welding procedures. For example, it is possible to weld gray iron, although it is problematic due to its high carbon content [2] [3].

Gray irons containing 2.0% to 4.5% C are called cast irons. However, cast iron used for industrial purposes generally contains 2% to 4.5% C, 1% to 3% Si, 0.02% to 0.75% P, 0.02% to 0.20% S, and 0.25% to 1.50% Mn. Cast iron alloys may also contain other elements deliberately added to obtain desired properties such as strength, hardness, hardenability, or corrosion resistance for specific applications. Common alloying elements are chromium, copper, molybdenum, and nickel. One of the distinguishing characteristics of gray iron is that the carbon is generally found as graphite, taking irregular shapes known as flakes [2] [4] [5].

Cast iron has a lower melting point than steel (1585˚C), between 1150˚C and 1250˚C. It has a higher fluidity than steel in the liquid state, and undergoes moderate shrinkage during solidification and cooling. These physical characteristics facilitate better molding to obtain parts with complex shapes. Gray iron is used in various industrial fields; however, the ductility of cast iron is much lower than that of steel [6] [7] [8]. This property restricts the applications. The mechanical properties depend on the microstructure, as well as the form of distribution of free graphite. The number, size, and shape of the graphite flakes affect the strength and ductility of the cast iron. Therefore, cast iron can be classified by the characteristics of graphite. There are four basic types of cast iron: gray iron, malleable iron, nodular iron, and white iron [2] [3] [4].

Gray iron microstructure consists of graphite flakes in a matrix of pearlite, ferrite, or both. This type of cast iron gets its name from the gray appearance of its fractured surface. Gray iron is the most common type of iron, being basically an iron-carbon-manganese-silicon alloy with 2.5% - 4.5% carbon. To minimize the formation of massive carbides and martensite with high carbon content, the graphite must be in a spheroidal form with a low surface-to-volume ratio. Ductile iron contains graphite in spheroidal form and therefore has better ductility; therefore, this type of cast iron has superior weldability to any other type. As the superficial area of the graphite in contact with the austenite matrix decreases, the

amount of carbon in the microstructure can decrease at room temperature. Graphite flakes contained in gray iron show the greatest tendency to dissolve in austenite due to their relatively large surface area. Therefore, gray cast iron is inherently brittle and often cannot withstand the shrinkage stresses that arise from fusion welding. Since graphite flakes cause lack of ductility, gray iron containing large graphite flakes is more brittle and less weldable than those with graphite nodules or small flakes [8] [9].

Cast iron applications are very diverse; they have advantage of being, in general, much easier to machine than steels. Mechanical characteristics of gray cast iron are its high compressive strength (50 to 100 MPa), its tensile strength, from 12 to 90 MPa, a good wear resistance and easily vibration absorption. As the melting temperatures of gray iron castings are low compared to that of steels, they have greater fluidity and less contraction when solidifying, which allows the production of pieces with thin thicknesses [8] [10] [11].

Gray iron has common problems that affect weldability; namely 1) high carbon content 2) lower ductility 3) high content of phosphorus, sulfur and oxygen 4) casting defects, and 5) impregnated oil. The welding process causes carbon to diffuse into the filler metal and/or Heat Affected Zone (HAZ), causing increased hardness and brittleness, which can lead to post-weld cracking. Graphite lamellae can dissolve during welding and precipitate as high-carbon martensite [12] [13] [14].

The objective of this study is to determine the effects caused by the welding process using the filler metal method with a 308 stainless steel coated electrode. It is a union between two dissimilar metals, followed by rapid cooling, which causes structural changes at the HAZ of the gray cast iron and the filler metal. Electric arc welding with covered electrode is the most used welding process which was applied in this research according to the AISI 304 stainless steel welding procedure [15]. Welding implies mixing of the consumable and the base metal which leads to alterations of the composition, the microstructure and the properties of the resulting surface layer as compared to the pure consumable [16].

## 2. Materials and Methods

Three gray cast iron specimens with the following composition were used: 2.43% C; 1.35% Si; 0.62% Mn, 0.15% S; 0.25% P to be welded with AISI 304 stainless steel. As filler metal E-308-16 flux-coated electrode was selected, which imparts gray cast iron mechanical and metallurgical properties at the seam. Specimen dimensions are shown in **Figure 1**.

The electric arc welding technique was used with a CD Hobart brand equipment, 400 A capacity. Welding process parameters were 90 A DC PI. Welded specimens were cooled rapidly in water.

After cooling, specimens were subjected to a tensile strength test. The tension test was performed by an Instron model 600DX universal testing machine.

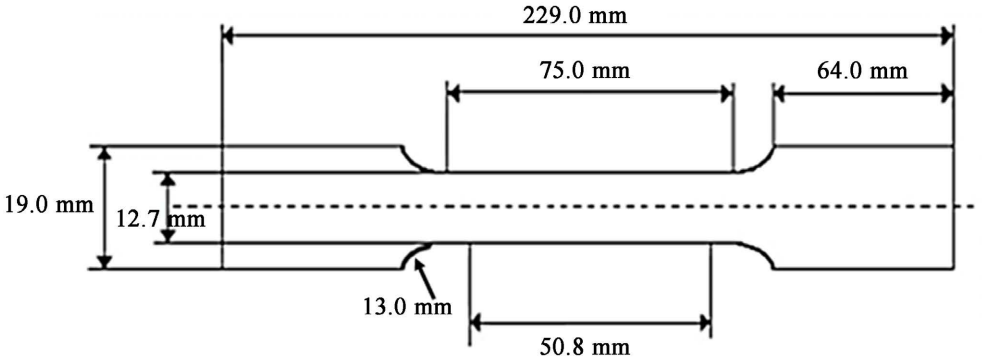


**Figure 1.** Dimensions of tensile test specimens.

Specimens were prepared according to **Figure 1**. Each test was carried out in 17 min total elapsed time, 32 s average.

After that, Vickers micro hardness was tested by a Wolpert brand equipment, model HS 250. The distance between each two indentations was 0.317 mm; 101 values were obtained from each sample; applying a 19.61 N load, at the base metal (grey cast iron), AISI 304, filler metal, and HAZ.

Metallographically prepared welded samples were analyzed by an Olympus metallographic microscope, model MG. Metallurgical microstructure was obtained at base metals, filler metal, and HAZ.

## 3. Results

Different investigations of the joining of dissimilar materials such as stainless steel and different castings have been carried out, but rapid cooling immediately after welding has not been considered. This research work is important because it allows us to analyze the possibility of recovering pieces of dissimilar materials by welding or, failing that, to determine if this may or may not be possible. To determine the effect of the cooling conditions, Vickers microhardness tests, metallography and tensile strength tests were carried out.

### 3.1. Vickers Microhardness

**Figure 2** shows the Vickers hardness profile, where hardness variations are observed among different zones of welded samples. The hardness average was 230.29 HV, the minimum hardness in both base metals was 167 HV, and the maximum 285 HV corresponded to the filler metal.

### 3.2. Metallographic Analysis

**Figure 3** shows metallurgical microstructures. **Figure 3(a)**, Gray cast iron, graphite type A (not etched sample), **Figure 3(b)** Gray cast iron, etched with Nital 5%, pearlitic matrix with some ferrite. **Figure 3(c)** AISI 304 stainless steel, austenite microstructure.

Significant changes of metallurgical microstructure were observed, mainly at the gray iron HAZ as shown in **Figure 4(a)** and **Figure 4(c)**, as well at the filler

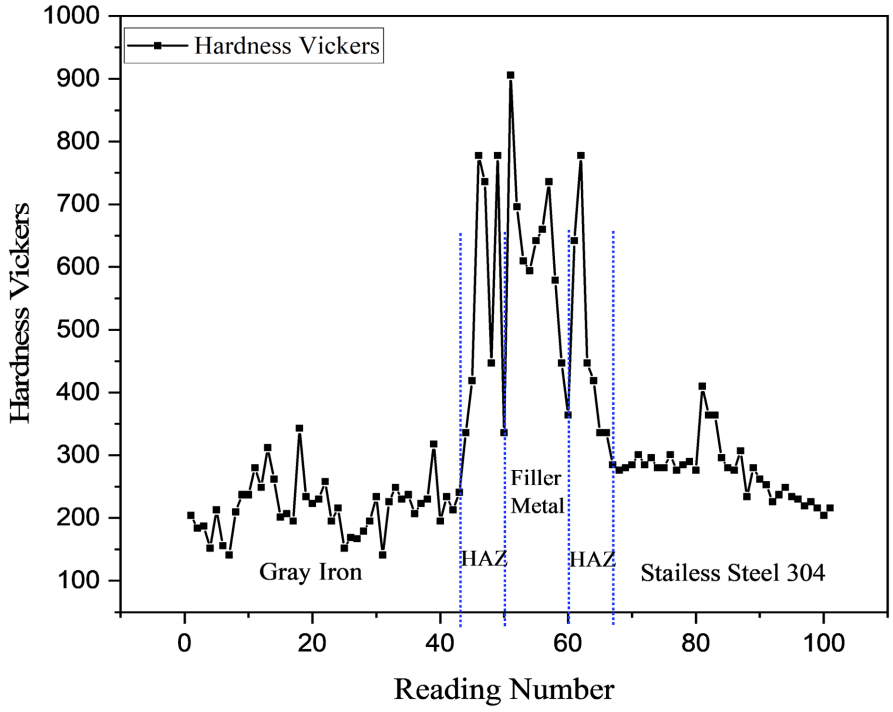


**Figure 2.** Average Vickers hardness profile of the welded samples studied.

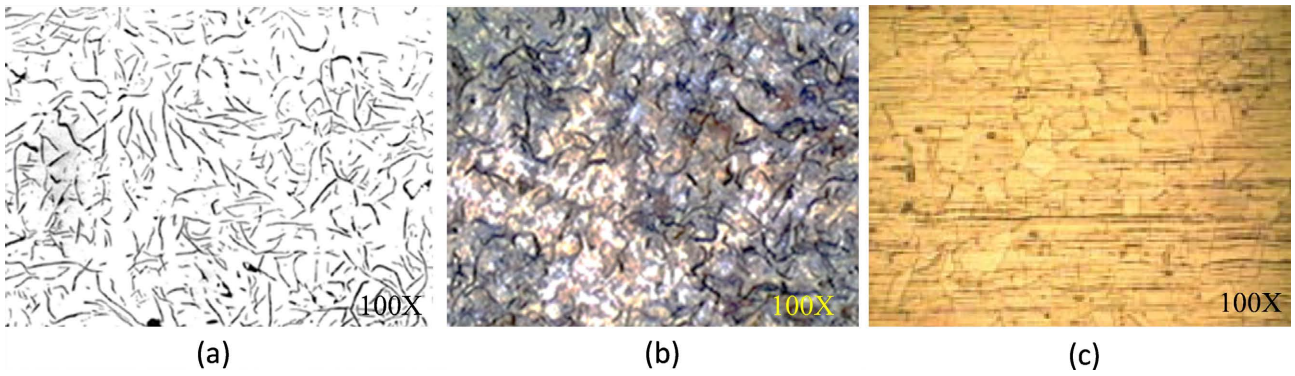


**Figure 3.** Metallurgical microstructures. (a) Sample not etched, graphite type A. (b) Sample etched with Nital, pearlitic matrix and some ferrite. (c) AISI 304 stainless steel, austenitic structure. 100× magnification.

metal illustrated in **Figure 4(b)** and **Figure 4(d)**. In HAZ a martensitic structure with retained austenite is observed, as a result of the fast cooling after the welding process. The filler metal microstructure consisted mainly of martensite, due to the fact that there was a carbon diffusion to the filler metal during the melting of the welding process.

In **Figure 5** the metallurgy microstructure is observed at 400×, **Figure 5(a)** shows a mixture of structures, coarse martensite and austenite, as well as the formation of ledeburite. **Figure 5(b)** coarse martensite with retained austenite, and crack formation caused by rapid cooling after welding. In **Figure 5(c)** a structure of coarse martensite and retained austenite is observed. **Figure 5(d)** shows more noticeable the presence of coarse martensite, retained austenite and ledeburite; as well as the presence of cracks, caused by the fast cooling after

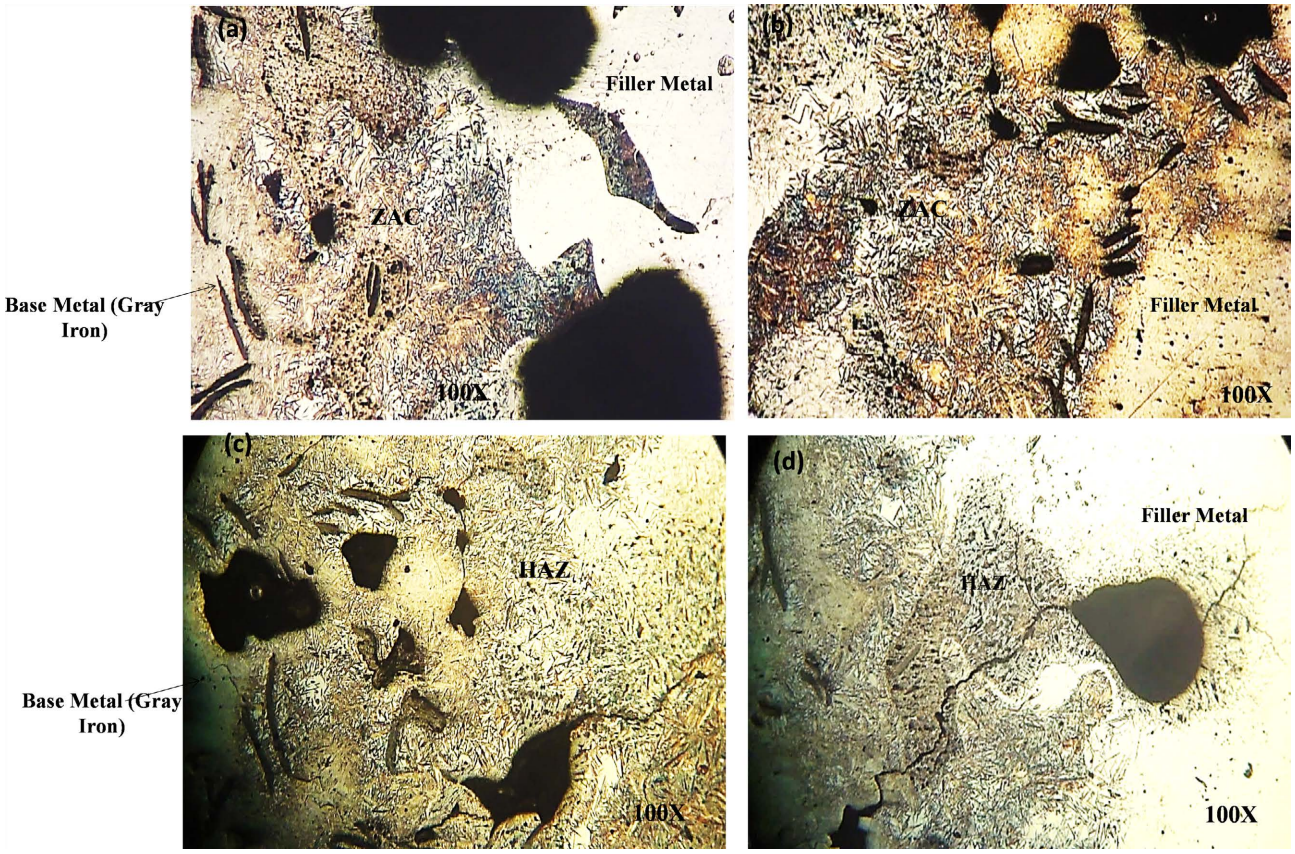


**Figure 4.** Metallurgical microstructures after welding process and fast cooling. (a) and (c) Gray iron HAZ. (b) and (d) Filler metal. 100× magnification.

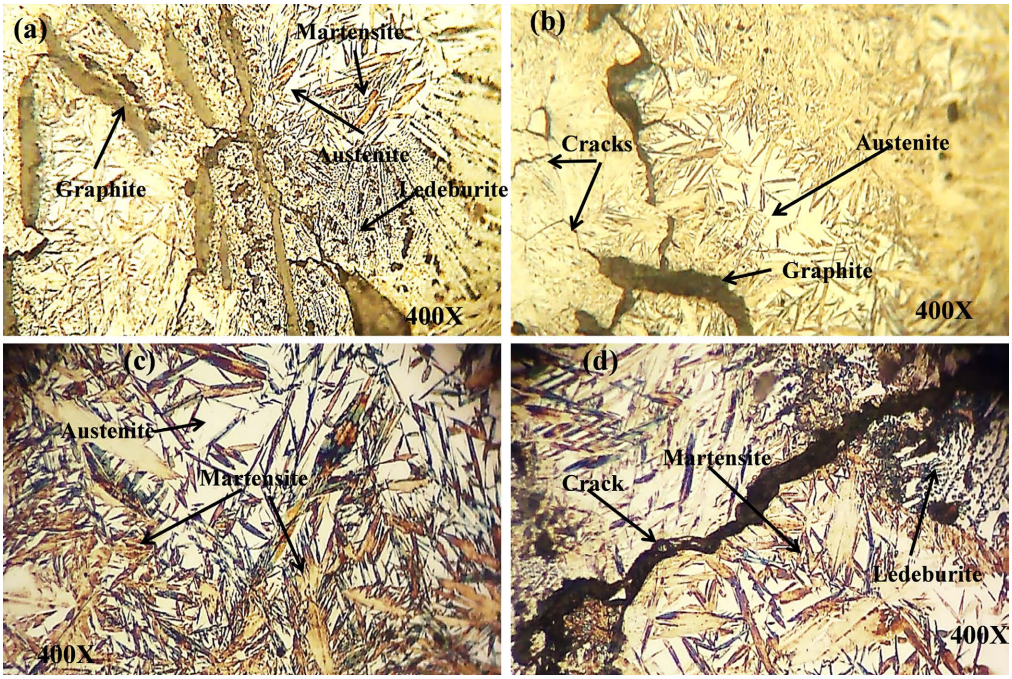


**Figure 5.** Metallurgical microstructures after welding process and fast cooling. (a) Coarse martensite, retained austenite and ledeburite. (b) Austenite and cracks. (c) Coarse martensite and retained austenite. (d) Martensite, ledeburite and cracks. 400× magnification.

welding process.

### 3.3. Tensile Strength Test

Table 1, are shown the average of the Tension test results carried out on the welded samples studied, as well as, in Figure 6.

## 4. Discussion

The investigations of the welding process between dissimilar materials with the

Table 1. Tension test result of welded samples

| Properties | Result |
|---|---|
| Maximum Load | 16.64 KN |
| Yield Strength | 0 |
| Tensile Strength | 294.20 MPa |
| Specimen length gauge | 50.80 mm/N |
| Gage length | 50.80 mm |
| End length | 52.16 |
| Total deformation | 1.36 mm |
| Strain $\varepsilon$ | 0.02677 mm/mm |
| Area under the curve | 20.023 J |

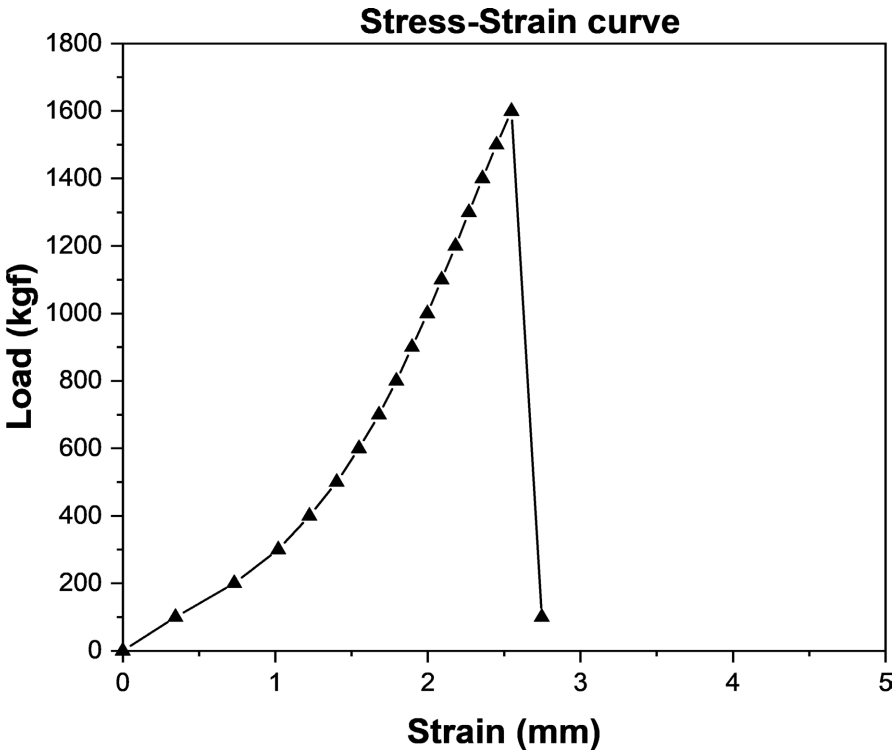


Figure 6. Stress-Strain curve representative of the specimens analyzed after welding and fast cooling.

focus on foundries or cast irons, have focused mainly on the welding of stainless steels and nodular irons, due to the better characteristics and properties of nodular cast iron, avoiding rapid cooling. [12] or through controlled cooling [14], little has been written about welding between gray cast iron and stainless steel, research has been done to recover corrosion losses in gray cast iron parts, adding stainless steel through the process of welding mediate filler material [16]. This work shows the effect of welding between two dissimilar materials, gray cast iron and E308-16 stainless steel, considering the parameters of the welding process but also the effect of rapidly cooling the pieces after joining them through the filler material process, the results are indicative of how the mechanical properties can vary as a result of the metallurgical changes of its microstructure caused by rapid cooling in water, immediately after welding. The significant variation in hardness was the result of rapid quenching in water after welding. Rapid cooling in water after welding also had an effect on changes in the metallurgical microstructure.

The metallographic analysis showed different metallurgical structures. The gray iron base metal consisted mainly of pearlite and some ferrite, and type A graphite. The microstructure of the HAZ was martensitic, retained austenite and ledeburite, with the presence of cracks as a result of rapid cooling after the welding process. The microstructure of the filler metal was mainly martensite, due to the diffusion of carbon to the filler metal in the welding process. In the AISI 304 base metal, the microstructure was only austenite. Microstructural differences across the welded areas were the result of the cooling rate and temperature differences across the samples during the welding process. The ledeburite eutectic structure was the result of melting during the welding process. The cracks were produced by quenching after welding.

The tensile test results in **Table 1** showed brittle behavior, as confirmed by the stress-strain curve in **Figure 6** without any plastic behavior.

## 5. Conclusions

Hardness variations along several zones of analyzed samples were directly related to different metallurgical structures as a result of cooling speed differences.

The most predominant HAZ structure was the very tetragonal martensite, which was due to very high tensile stresses after the welding process and the high cooling speed, which caused crack formation.

According to the hardness result, the higher resistance was at the HAZ, similar to the Filler Metal, due to the changes in the metallurgical structure as a consequence of the welding process and the cooling speed in the samples.

The results obtained show the effect of the welding process and its subsequent cooling in water, this practice limits its application at an industrial level, due to the fact that very controlled conditions must be maintained to do so, other less severe cooling means should be investigated and the results compared.

## Conflicts of Interest

The authors declare no conflicts of interest regarding the publication of this paper.

## References


[1] Cary, H.B. (1998) The History of Welding. In: Modern Welding Technology, Prentice Hall, Hoboken.

[2] Olson, D.L., Siewert, T.A., Liu, S. and Edwards, G.R. (1993) ASM Handbook Volume 6: Welding, Brazing and Soldering, 10th Edition, ASM International, Materials Park. https://doi.org/10.31399/asm.hb.v06.9781627081733

[3] Pascual, M., Cembrero, J., Salas, F. and Pascual-Martines, M. (2008) Analysis of the Weldability of Ductile Iron. *Materials Letters*, **62**, 1359-1362. https://doi.org/10.1016/j.matlet.2007.08.070

[4] Ospina López, R., Aguirre Corrales, H. and Parral, H. (2007) Soldabilidad en aceros inoxidables y aceros disimiles. *Scientia et Technica*, **1**, 273-278.

[5] El-Shennawy, M. and Omar, A. (2010) Similar and Dissimilar Welding of Ductile Cast Iron. In: Hinduja, S. and Li, L., Eds., *Proceedings of the* 36*th International MATADOR Conference*, Springer, London, 297-302. https://doi.org/10.1007/978-1-84996-432-6_68

[6] Peckner, D. and Bernstein, I.M. (1977) Handbook of Stainless Steels. McGraw-Hill, New York.

[7] Phillips, D.H. (2016) Welding Engineering: An Introduction. Wiley, Hoboken. https://doi.org/10.1002/9781119191407

[8] Pascual, M., Ferrer, C. and Rayón, E. (2009) Weldability of Spheroidal Graphite Ductile Cast Iron Using Ni/Ni-Fe Electrodes. *Revista de Metalurgia*, **45**, 334-338. https://doi.org/10.3989/revmetalm.0814

[9] Winarto, G.D., Wardhani, R. and Syarif, I. (2014) Analysis of Buttering Method on Mechanical Properties Welded Material Low Carbon Steel. *IPTEK, Journal of Proceeding Series*, **1**. https://doi.org/10.12962/j23546026.y2014i1.386

[10] Doyle, L.E. (1998) Procesos de materiales de manufactura para ingenieros. 3rd Edition, Prentice Hall, México.

[11] Industrial Applications for Dissimilar Metal Welding. SPI Lasers. https://www.spilasers.com/application-welding/industrial-applications-dissimilarmetal-welding

[12] Sehsah, A.M., Ghanem, M.M., Abdel-Aleem, H.A. and El-Shennawy, M. (2021) Dissimilar Welding of Ductile Cast Iron to 304 Stainless Steel. *International Journal of Mechanical Engineering* (*IJME*), **10**, 35-48.

[13] Carrasco, J.C., Vicente, F.S., Corral, A.M. and Guillamó, M.P. (2022) Weldability of Ductile Cast Iron Using AISI-316L Stainless Steel ER Rod. *Revista de Metalurgia*, **58**. https://doi.org/10.3989/revmetalm.224

[14] El-Banna, E.M. (1999) Effect of Preheat on Welding of Ductile Cast Iron. *Materials Letters*, **41**, 20-26. https://doi.org/10.1016/S0167-577X(99)00098-1

[15] García-Lira, J., Curiel-Reyna, E., Curiel-Razo, Y., Lara-Guevara, A. and Rojas-Rodríguez, I. (2021) Characterization of Dissimilar Welding between 304 Stainless Steel and Gray Iron Using Nickel Coated Electrode. *Materials Sciences and Applications*, **12**, 614-621. https://doi.org/10.4236/msa.2021.1212041

[16] Heider, B., Oechsner, M., Reisgen, U., Ellermeier, J., Engler, T., Andersohn, G.,

Sharma, R., Gonzalez Olivares, E. and Zokoll, E. (2020) Corrosion Resistance and Microstructure of Welded Duplex Stainless Steel Surface Layers on Gray Cast Iron. *Journal of Thermal Spray Technology*, **29**, 825-842.
https://doi.org/10.1007/s11666-020-01003-y